

# An Antisense CAG Repeat Transcript at *JPH3* Locus Mediates Expanded Polyglutamine Protein Toxicity in Huntington's Disease-like 2 Mice

Brian Wilburn,<sup>1</sup> Dobrila D. Rudnicki,<sup>2,8</sup> Jing Zhao,<sup>3,8</sup> Tara Murphy Weitz,<sup>1</sup> Yin Cheng,<sup>3</sup> Xiaofeng Gu,<sup>1</sup> Erin Greiner,<sup>1,4</sup> Chang Sin Park,<sup>1</sup> Nan Wang,<sup>1</sup> Bryce L. Sopher,<sup>5</sup> Albert R. La Spada,<sup>5,6</sup> Alex Osmand,<sup>7</sup> Russell L. Margolis,<sup>2</sup> Yi E. Sun,<sup>3</sup> and X. William Yang<sup>1,\*</sup>

<sup>1</sup>Department of Psychiatry and Biobehavioral Sciences, Center for Neurobehavioral Genetics, Semel Institute for Neuroscience and Human Behavior, Brain Research Institute, David Geffen School of Medicine, University of California, Los Angeles, Los Angeles, CA 90095, USA

<sup>2</sup>Division of Neurobiology, Laboratory of Genetic Neurobiology, Department of Psychiatry, Johns Hopkins University School of Medicine, Baltimore, MD 21287, USA

<sup>3</sup>Department of Psychiatry and Biobehavioral Sciences, Department of Pharmacology, Mental Retardation Research Center, Semel Institute for Neuroscience and Human Behavior, Brain Research Institute, David Geffen School of Medicine, University of California, Los Angeles, Los Angeles, CA 90095, USA

<sup>4</sup>Department of Chemistry and Biochemistry, University of California, Los Angeles, Los Angeles, CA 90095-1569, USA

<sup>5</sup>Department of Laboratory Medicine, University of Washington Medical Center, Seattle, WA 98195, USA

<sup>6</sup>Departments of Pediatrics and Cellular and Molecular Medicine, Division of Biological Sciences, Institute for Genomic Medicine, University of California, San Diego, La Jolla, CA 92093, USA and Rady Children's Hospital, San Diego, CA 92123, USA

<sup>7</sup>Department of Medicine, University of Tennessee Graduate School of Medicine, Knoxville, TN 37920, USA

<sup>8</sup>These authors contributed equally to this work

\*Correspondence: [xwyang@mednet.ucla.edu](mailto:xwyang@mednet.ucla.edu)

DOI 10.1016/j.neuron.2011.03.021

## SUMMARY

Huntington's disease-like-2 (HDL2) is a phenocopy of Huntington's disease caused by CTG/CAG repeat expansion at the *Junctophilin-3* (*JPH3*) locus. The mechanisms underlying HDL2 pathogenesis remain unclear. Here we developed a BAC transgenic mouse model of HDL2 (BAC-HDL2) that exhibits progressive motor deficits, selective neurodegenerative pathology, and ubiquitin-positive nuclear inclusions (NIs). Molecular analyses reveal a promoter at the transgene locus driving the expression of a CAG repeat transcript (*HDL2-CAG*) from the strand antisense to *JPH3*, which encodes an expanded polyglutamine (polyQ) protein. Importantly, BAC-HDL2 mice, but not control BAC mice, accumulate polyQ-containing NIs in a pattern strikingly similar to those in the patients. Furthermore, BAC mice with genetic silencing of the expanded CUG transcript still express *HDL2-CAG* transcript and manifest polyQ pathogenesis. Finally, studies of HDL2 mice and patients revealed CBP sequestration into NIs and evidence for interference of CBP-mediated transcriptional activation. These results suggest overlapping polyQ-mediated pathogenic mechanisms in HD and HDL2.

## INTRODUCTION

Huntington's disease-like-2 (HDL2) is an autosomal dominant neurodegenerative disorder that has a broad phenotypic overlap

with Huntington's disease (HD) (Margolis et al., 2001). Similar to HD, HDL2 is characterized by adult onset of symptoms including chorea, dystonia, rigidity, bradykinesia, psychiatric symptoms, and dementia, eventually leading to premature death about 10–15 years after disease onset (Margolis et al., 2005). HDL2 accounts for a small subset of patients with clinical manifestations of HD who do not have the HD mutation, an expanded CAG repeat-encoding polyglutamine (polyQ) repeat in huntingtin (Margolis et al., 2001, 2004; Schneider et al., 2007).

The neuropathology of postmortem HDL2 brains is strikingly similar to that of HD (Greenstein et al., 2007; Rudnicki et al., 2008). Both exhibit robust and selective striatal and cortical atrophy with neurodegeneration primarily targeting the striatal medium spiny neurons (MSNs) and a subset of cortical pyramidal neurons (Greenstein et al., 2007; Rudnicki et al., 2008). Moreover, both HD and HDL2 brains contain intranuclear inclusions (NIs) that are ultrastructurally similar and are immunostained with ubiquitin and 1C2 (an antibody against the expanded polyQ epitope that can also recognize polyleucine; Trotter et al., 1995; Dorsman et al., 2002). The pattern of NI distribution in HD and HDL2 is similar, but not identical. They both have a higher density in the cortex and amygdala than in the striatum and NIs are rarely observed in the cerebellum or midbrain (Greenstein et al., 2007; Rudnicki et al., 2008). However, unlike those in HD, NIs in HDL2 are more frequent in the upper cortical layers II/III than deep cortical layers, and they are absent in the pons and medulla (Greenstein et al., 2007; Rudnicki et al., 2008). Another key pathological difference between the two disorders is that NIs in HD, but not those in HDL2, contain mutant huntingtin (mhtt) (Margolis et al., 2001). Therefore, the pathogenic origin of NIs in HDL2 remains to be uncovered.

HDL2 is caused by a CTG/CAG expansion on chromosome 16q24.3 (Holmes et al., 2001). The expanded CTG/CAG repeats

in HDL2 patients range from 40–59, with normal individuals carrying 6–28 repeats. HD and HDL2 not only have comparable ranges of CTG/CAG repeat expansions, but also similar slopes in their inverse relationships between the repeat length and age of onset for movement disorders (Margolis et al., 2004). The CTG repeat expansion is located within the variably spliced exon 2A of *JPH3*, which is not part of the main transcript encoding JPH3 protein (Holmes et al., 2001). On the sense strand, three splice variants that include exon 2A have been described, placing the expanded CTG repeat in poly-leucine or poly-alanine open reading frames (ORFs) or in the 3' untranslated region (UTR).

Currently, the molecular pathogenic mechanisms for HDL2 remain an enigma (Margolis et al., 2005; Orr and Zoghbi, 2007). Three possible mechanisms have been postulated. First, the expansion of the CUG repeat may reduce *JPH3* mRNA expression leading to a partial loss of function for JPH3 protein, which normally tethers the plasma membrane to the endoplasmic reticulum to facilitate crosstalk between cell surface and intracellular ion channels (Nishi et al., 2002; Takeshima, 2001). In support of this theory, *JPH3* knockout mice exhibit motor impairment but such mice do not appear to accumulate NIs or exhibit neurodegeneration (Nishi et al., 2002). A second possible pathogenic mechanism, similar to that demonstrated for myotonic dystrophy types 1 and 2 (DM1 and DM2), is that the expanded CUG or CCUG repeat RNA form RNA foci which can sequester an RNA binding protein muscleblind-like 1 (MBNL1) and interfere with its function in regulating alternative splicing (Ranum and Cooper, 2006; Kanadia et al., 2003). Supporting this possibility, Rudnicki and colleagues (Rudnicki et al., 2007) showed CUG RNA foci in HDL2 brains and the ability of mutant *HDL2-CUG* RNA transcripts to interfere with the splicing of MBNL1 targets in cultured cells. However, the expanded CUG RNA in DM1 was not known to elicit NIs or apparent neurodegeneration. Moreover, CUG RNA foci in HDL2 patients do not frequently colocalize with NIs (Rudnicki et al., 2007), suggesting distinct pathogenic origins for these entities.

To gain insight into the pathogenesis of an HD phenocopy, we developed a series of bacterial artificial chromosome (BAC)-mediated transgenic mouse models of HDL2 (BAC-HDL2) that contain an expanded CTG/CAG repeat in the human *JPH3* BAC, as well as control BAC mice with a nonexpanded CTG/CAG repeat. BAC-HDL2, but not control BAC, mice recapitulate motor, neuropathological, and molecular phenotypes similar to those in the patients. Importantly, molecular analyses revealed a promoter driving the expression of an expanded CAG repeat-containing transcript emanating from the strand antisense to *JPH3*. This mutant HDL2-CAG transcript can mediate polyQ protein toxicity (e.g., sequestration and interference of CREB binding protein [CBP]-mediated transcription), hence providing a molecular pathogenic link between HD and HDL2.

## RESULTS

### Generation and Characterization of a BAC Transgenic Mouse Model of HDL2

Because BACs preserve the intact human genomic context and have been successfully used to develop transgenic mouse

models for other neurodegenerative disorders including HD (Gong et al., 2002; Yang et al., 1997; Gray et al., 2008; Gu et al., 2009), we undertook a BAC transgenic approach to develop a mouse model for HDL2. We selected a human BAC (RP11-33A21) that contains the intact 95 kb *JPH3* genomic locus in addition to approximately 30 kb 5'- and 40 kb 3'-genomic flanking sequences. The BAC was engineered to contain an expanded CTG/CAG track of 120 repeats in exon 2A of *JPH3*, preserving the repeat ORFs in both the sense and antisense strands compared to those in the patients (Figure 1A). In designing the BAC-HDL2 construct, we purposely chose a longer stretch of CTG/CAG repeats (~120 repeats) than what is found in patients (i.e., 40–59 repeats) because prior experience in modeling other trinucleotide repeat disorders such as SCA1 and HD suggests that longer repeat lengths are needed to accelerate the disease process such that disease manifestation occurs within the short lifespan of a mouse (Zoghbi and Botas, 2002).

The engineered mutant BAC was microinjected into inbred FvB/N mouse embryos to generate transgenic founders. A total of ten BAC-HDL2 founders were obtained and five were bred for germline transmission. Three of the BAC-HDL2 lines (C, F, and M) integrated one to four copies of the BAC transgene (data not shown). Direct sequencing was used to determine the precise repeat length: C line has 116 CTG/CAG repeats, F line has 122 repeats, and M line has integration at a single locus of BAC with 119 and 13 repeats. Because both C and F lines have only the expanded repeats, we focused our phenotypic studies on these two independent lines. We next assessed whether *JPH3* mRNA and JPH3 protein are overexpressed in these models. As demonstrated in Figure 1B, reverse transcriptase PCR (RT-PCR) analysis that specifically amplified exon 2B to exon 4 of *JPH3* readily detects transgene expression in the brain of BAC-HDL2 lines. Semiquantitative RT-PCR (sqRT-PCR) analyses revealed that the level of overexpression was about 100% of endogenous murine *Jph3* in the C line and about 20% in the F line (Figure S1, available online). Intriguingly, when we analyzed BAC-HDL2 lines for JPH3 protein levels, we did not detect any significant overexpression (Figure 1C and Figure S1). Nonetheless, the latter observation is consistent with the finding in DM1 that the expanded CUG repeat may impair DMPK protein expression via a *cis* mechanism of reduced RNA nuclear export (Ranum and Cooper, 2006). Because of the higher level of transgene expression in the BAC-HDL2-C line, the majority of our phenotypic analyses are focused on this line (hereafter referred to as BAC-HDL2). However, several pathogenic phenotypes were also independently confirmed by using the F line (BAC-HDL2-F).

### BAC-HDL2 Mice Exhibit Age-Dependent Motor Deficits and Neurodegenerative Pathology

HDL2 patients are characterized clinically by a middle-aged onset of movement disorders including motor incoordination (Margolis et al., 2005) and neuropathologically by the selective atrophy of the striatum and cortex (Greenstein et al., 2007; Rudnicki et al., 2008). To evaluate whether our model recapitulates aspects of these disease features, we studied a cohort of BAC-HDL2 mice and wild-type littermates by using the

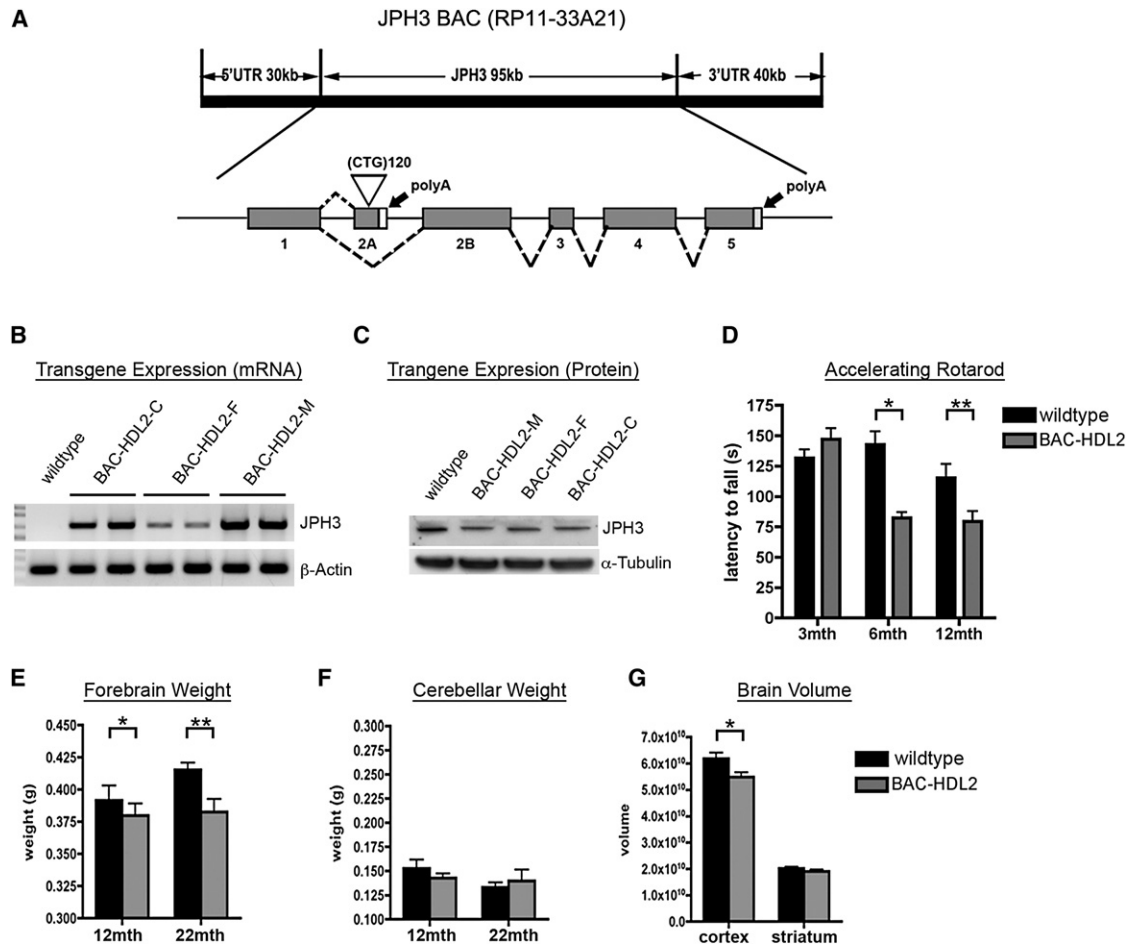


**Figure 1. Generation and Characterization of BAC-HDL2 Animals**

(A) A schematic representation of the human *JPH3* locus. A BAC containing the intact JPH locus (RP11-33A21) was modified in order to insert ~120 CTG repeats into the alternatively spliced exon 2A (white triangle).

(B) RT-PCR was performed by using primers specific to human *JPH3* exons 2B and 4.

(C) *JPH3* western blot was performed on brain lysates isolated from BAC-HDL2 C/M/F lines and wild-type control.

(D) Accelerating rotarod testing was performed at 3, 6, and 12 months old (3 months: wild-type, n = 22; BAC-HDL2, n = 16; 6 months: wild-type, n = 14 and BAC-HDL2, n = 11; 12 months: wild-type, n = 10; BAC-HDL2, n = 11).

(E) BAC-HDL2 forebrains weigh significantly less than their wild-type littermates at both 12 and 22 months old.

(F) No significant differences were detected in cerebellum weights between BAC-HDL2 and its wild-type littermates at 12 and 22 months old.

(G) Stereological brain volume measurements of BAC-HDL2 cortex and striatum revealed a significant decrease in the cortical volume at 18–22 months old (BAC-HDL2: striatum, n = 6; cortex, n = 6; wild-type: striatum, n = 6, cortex, n = 6). Values are mean  $\pm$  SEM (\*p < 0.05, \*\*p < 0.01, Student's t test).

behavioral and neuropathological assays that have been established for HD mice (Gray et al., 2008). To assess evidence of age-dependent motor deficits, we used accelerating rotarod assay and observed significant impairment in BAC-HDL2 mice compared to wild-type controls at both 6 and 12 months old, but not at 3 months old (Figure 1D). Statistical analyses by using a general linear model with repeated-measures two-way ANOVA revealed an effect of time ( $F_{2,30} = 8.728$ ,  $p = 0.001$ ) and genotype ( $F_{1,15} = 4.651$ ,  $p = .048$ ) on rotarod performance as well as a significant time/genotype interaction (Figure 1E) ( $F_{2,30} = 14.822$ ,  $p < 0.001$ ). One-way ANOVA analysis revealed that latency to fall significantly decreased in BAC-HDL2 mice over time ( $F_{2,37} = 19.047$ ,  $p < 0.001$ ), while no such change was observed in

wild-type littermates. These results reveal that BAC-HDL2 mice exhibit progressive motor deficits when compared to their wild-type littermate controls.

To assess whether BAC-HDL2 mice also exhibited evidence of neurodegenerative pathology, we weighed the forebrain and cerebellum at 12 and 22 months old, an assay that is able to detect selective forebrain atrophy in BACHD mice (Gray et al., 2008). As shown in Figures 1E and 1F, we observed a significant decrease in forebrain weight, but not cerebellar weight, in BAC-HDL2 mice as compared to wild-type controls. No difference in forebrain weight was detected at 3 months old (data not shown). To more precisely quantify forebrain atrophy, we performed unbiased stereology by using 18- to 22-month-old

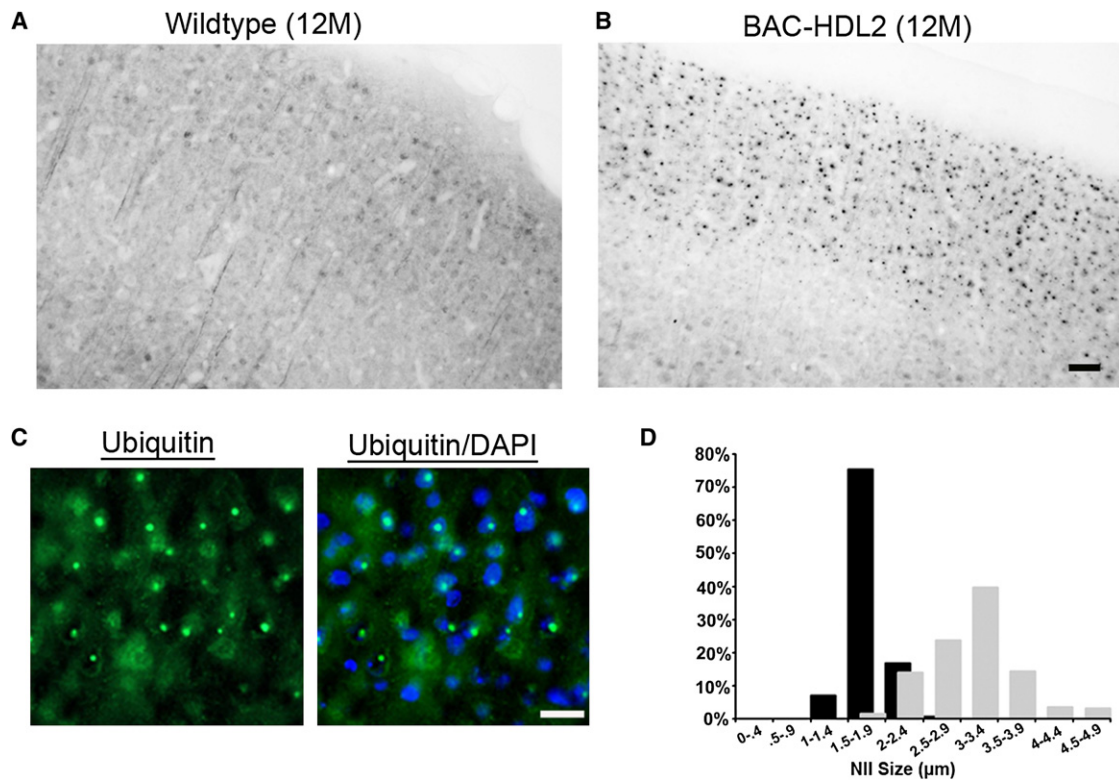


**Figure 2. Ubiquitin-Immunoreactive Nuclear Inclusions in BAC-HDL2 Brains**

(A and B) Antigen retrieval followed by immunohistochemical staining with 1C2 antibody. Twelve-month-old BAC-HDL2 brain sections revealed numerous large inclusion bodies in the cortical layers II/III (B). No such staining was observed in the respective brain regions in the wild-type animals (A).

(C) Ubiquitin-immunoreactive inclusion bodies in BAC-HDL2 brain are colocalized with the nuclear marker DAPI; hence, they are nuclear inclusions (NIs).

(D) Distribution of NI size in BAC-HDL2 mice at 3 and 12 months old with summary histograms shown. Mean = 1.8  $\mu\text{m}$  versus 3.13  $\mu\text{m}$  for 3 and 12 months old, respectively; \* $p < 0.001$ , Student's  $t$  test. BAC-HDL2: motor sensory (MS) cortex layers I/II/III at 3 months old (155 NIs measured in two mice) and 12 months old (194 NIs measured in two mice). Scale bar = 50  $\mu\text{m}$ .

BAC-HDL2 and control brains and found a significant reduction of cortical, but not striatal, volumes in BAC-HDL2 mice compared to the controls (Figure 1G). The latter finding may reflect a more slowly progressive neurodegenerative process in BAC-HDL2 striata. In summary, our behavioral and neuropathological studies reveal that BAC-HDL2 mice exhibit age-dependent motor deficits and neurodegenerative pathology consistent with those in HDL2.

#### BAC-HDL2 Mice Recapitulate Key Molecular Pathological Features of HDL2

We next addressed whether BAC-HDL2 mice also recapitulate the two molecular pathological hallmarks of HDL2, ubiquitin-positive NIs and CUG RNA foci that colocalize with MBNL1 (Greenstein et al., 2007; Rudnicki et al., 2007, 2008). As shown in Figure 2, we could readily detect prominent ubiquitin-immunoreactive inclusion bodies in BAC-HDL2, but not wild-type control, mice at 12 months old. Double fluorescent staining with an anti-ubiquitin antibody and DAPI demonstrated that the inclusion bodies were exclusively localized in the nucleus and hence were NIs (Figure 2C). Moreover, double immunostaining for ubiquitin and NeuN revealed that NIs were exclusively localized within neurons in BAC-HDL2 brains (data not shown). The

distribution of the NIs in the brains of BAC-HDL2 mice is remarkably similar to that in the patients (Figure S2A; Greenstein et al., 2007; Rudnicki et al., 2008). Ubiquitin-positive NIs were most abundant in the upper cortical layers, hippocampus (data not shown), and amygdala, with relatively low levels detected in the deep cortical layers and striatum. NIs were not detected in the cerebellum (Figure S2A), substantia nigra, thalamus, or brain stem (data not shown).

We next investigated whether the formation of NIs is progressive in BAC-HDL2 brains. NIs were absent in BAC-HDL2 brains at 1 month old, but could be readily detected in the cortex and hippocampus starting at 3 months old (data not shown). The size of NIs in BAC-HDL2 cortical neurons increases from an average diameter of 1.8  $\mu\text{m}$  at 3 months old to 3.13  $\mu\text{m}$  by 12 months old (Figure 2D). In summary, neuropathological analyses revealed that BAC-HDL2 mice recapitulate the progressive and brain region-specific formation of ubiquitin-positive NIs, a key pathological hallmark of HDL2.

The second pathological hallmark for HDL2 is the formation of CUG repeat-containing RNA foci that are independent of the NIs (Rudnicki et al., 2007). To assess whether 6-month-old BAC-HDL2 mice might also recapitulate such phenotype, we performed fluorescent in situ hybridization (FISH) with an

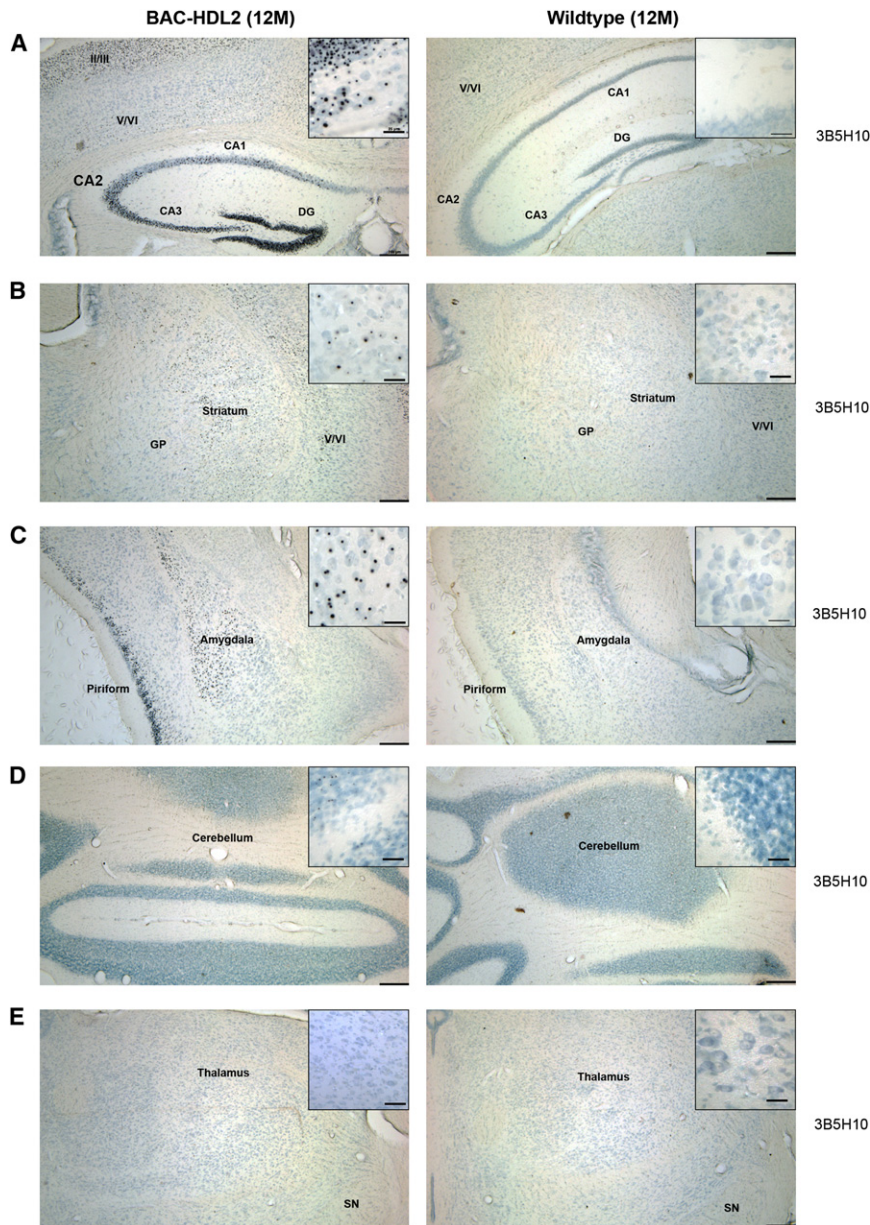


**Figure 3. The Distribution of 3B5H10-Immunoreactive NIs in BAC-HDL2 Brains Recapitulates that Seen in HDL2 Patients**

Immunostaining with a monoclonal antibody against expanded polyQ (3B5H10) in 12-month-old BAC-HDL2 and wild-type brain sections. Prominent 3B5H10-stained aggregates are detected in the mutant, but not wild-type, mouse brains in the upper cortical layers and hippocampus (A), striatum (B), and amygdala (C). Very few if any 3B5H10-immunoreactive aggregates were detected in the cerebellum (D) or thalamus (E). Scale bar = 200  $\mu$ m; inset scale bar = 25  $\mu$ m.

(Trottier et al., 1995), but can also recognize some normal long polyQ proteins such as TBP as well as some other amino acid stretches such as poly-leucine (Dorsman et al., 2002). Because of this latter possibility, the precise molecular nature of the 1C2 immunoreactivity within NIs in HDL2 remains to be clarified.

We next asked whether the NIs in BAC-HDL2 mice, like those in HDL2 patients, could be immunostained with 1C2. By using a sensitive antigen retrieval technique (Osmand et al., 2006) we were able to detect 1C2-immunoreactive NIs in 12-month-old BAC-HDL2 brains that are unlike the faint diffuse nuclear staining found in the wild-type controls (Figure S3A). Such 1C2 (+) NIs were not detected at 1 month old, but could be detected at 3 months old and became progressively enlarged at 6 and 12 months old (Figures S3A and S3C). Finally, double immunofluorescent staining revealed that 1C2-immunoreactive NIs colocalized with ubiquitin-positive NIs (Figure S3B), suggesting that the composition of NIs in BAC-HDL2 mice is quite similar to those described in HDL2 patients.

To provide further evidence that BAC-HDL2 NIs contain an expanded polyQ protein, we used another monoclonal antibody, 3B5H10, which has been shown to be specific to the expanded polyQ epitope in all known polyQ disorders (Brooks et al., 2004). Immunostaining with 3B5H10 after antigen retrieval revealed that NIs in 12-month-old BAC-HDL2 cortices and striatum were prominently stained with this expanded polyQ-specific antibody (Figure 3). No such 3B5H10 (+) NIs were detected in the brains of wild-type control littermates at 12 months old (Figure 3). Importantly, the distribution of 3B5H10-immunoreactive NIs in BAC-HDL2 brains is strikingly similar to that of patients, with prominent levels of NIs in the cortex (the upper cortical layers more than the deep cortical layers), hippocampus, and amygdala, decreased abundance in the striatum, and very few if any

established protocol (Rudnicki et al., 2007). We could readily detect CUG RNA foci in BAC-HDL2, but not wild-type, cortical sections (Figure S2B). Similar to those in HDL2 patients, the RNA foci were rarely colocalized with NIs and were colocalized with Mbn1 (Figure S2B). Thus, we concluded that BAC-HDL2 mice also recapitulate the phenotype of CUG RNA foci, another molecular pathological marker for HDL2.

#### **Evidence for Polyglutamine Protein Pathology in BAC-HDL2 Brains**

One intriguing finding in HDL2 neuropathology is the immunoreactivity of NIs with 1C2, a monoclonal antibody that has relatively high specificity to all expanded neuropathogenic polyQ proteins

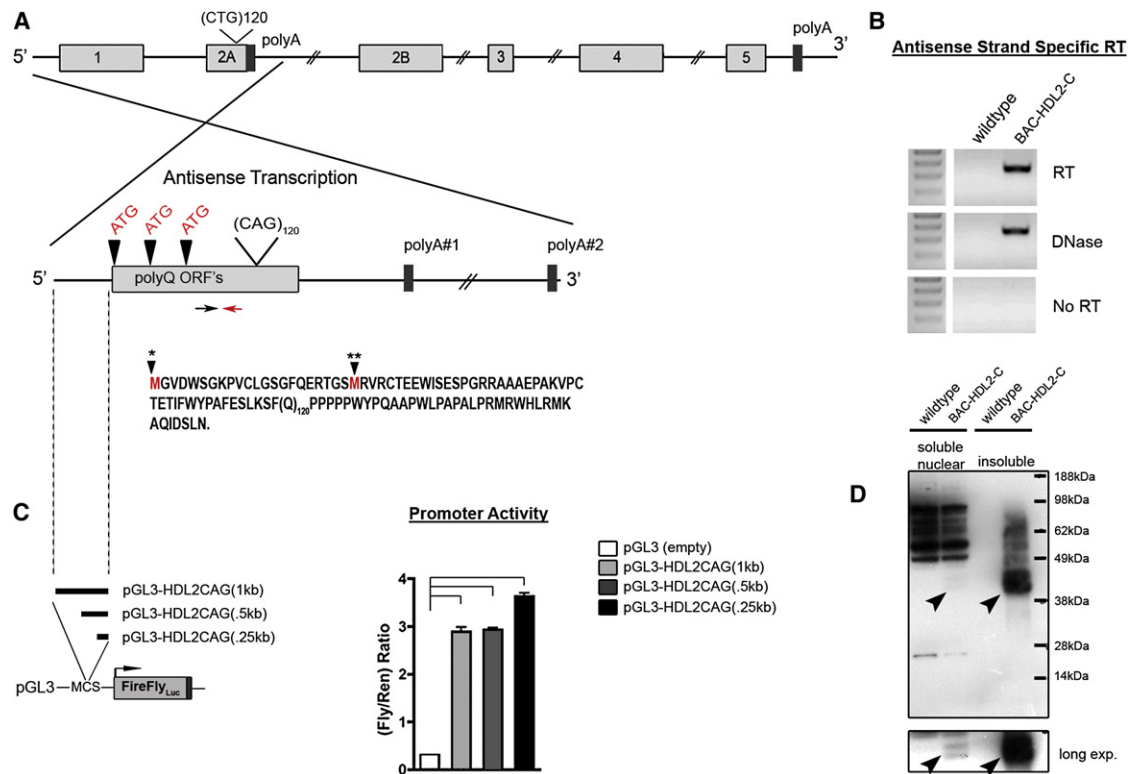


**Figure 4. Expression of Mutant HDL2-CAG RNA and Proteins in BAC-HDL2 Brains**

(A) Graphic representation of potential HDL2-CAG transcript(s) containing the expanded CAG repeat with polyQ ORFs (vertical arrowheads). The two closest polyA signals are shown. A red arrow marks the location of the primer used to drive reverse-strand-specific cDNA synthesis. The black arrow marks the location of the forward primer used for PCR after cDNA synthesis. Defined HDL2-CAG mutant transcripts include two potential ORFs through the CAG repeat (black arrowhead with asterisks) based on the differential usage of the two ATG translational initiation codons that can be amplified (the first ATG codon is not in any 5' RACE product).

(B) RT-PCR analyses provide evidence for the expression of HDL2-CAG transcripts emanating from the JPH3 antisense strand in BAC-HDL2 animals.

(C) DNA upstream of HDL2-CAG (position defined by dashed line) was cloned in front of luciferase in order to detect promoter activity in primary cortical neurons. Values are mean ± SEM (\*p < 0.01 for pGL3-HDL2CAG [1kb], pGL3-HDL2CAG [.5 kb], and pGL3-HDL2CAG [.25 kb] compared to empty vector, pGL3-empty).

(D) Western blot analysis with 3B5H10 antibody was performed on soluble nuclear soluble fractions as well as insoluble fractions extracted from the forebrain of BAC-HDL2 and wild-type 18-month-old mice. Black arrowheads point to disease-associated polyQ protein bands found specifically in BAC-HDL2 line brains, but not in wild-type littermate controls. This novel polyQ protein (termed HDL2-CAG) markedly accumulates in the insoluble fraction in the aged mutant brains.

NIs detected in the cerebellum, thalamus, and brain stem (Figure 4 and data not shown).

Taken together, our neuropathological studies with both 1C2 and 3B5H10 antibodies demonstrated that the NIs found in BAC-HDL2 brains recapitulate the patterns seen in HDL2 patients. Furthermore, an expanded polyQ protein is probably a component of such NIs.

### JPH3 BAC Transgenic Mice with Nonexpanded CTG/CAG Repeats Do Not Exhibit Evidence of Disease Pathogenesis

Because pathogenesis of HDL2 has been linked to the expansion of CTG/CAG repeats at the human JPH3 locus (Holmes et al., 2001), we next addressed whether disease pathogenesis in the BAC-HDL2 model, particularly the formation of NIs, could also be dependent on the repeat expansion in the BAC transgene. To test this hypothesis, we used two different wild-type JPH3 BAC transgenic control mice. The first control model

was generated in the FvB/N background by using the same wild-type BAC (RP11-33A21) as the one used to generate BAC-HDL2, except the CTG/CAG repeat length was 14. This control wild-type BAC construct was engineered to insert an enhanced green fluorescent protein (EGFP) within exon 1 of JPH3 (Figure S4A). The transgenic mouse line (termed BAC-JPH3) expressed EGFP as well as the nonexpanded CUG and CAG transcripts, but not JPH3 protein (Figure S1). This mouse line is an ideal control to address whether overexpression of non-expanded CUG- or CAG-containing mRNA transcripts from the JPH3 transgene locus could induce toxicity in vivo. To assess whether overexpression of any wild-type proteins encoded by the JPH3 sense strand transcripts could induce disease pathogenesis, we employed a second control mouse model. This control utilized a different BAC (CTD-2195P9) encompassing the intact human JPH3 genomic locus with 14 CTG/CAG repeats and was created and maintained in the C57/BL6 background (BAC-JPH3b6; Figure S4B). Expression analyses revealed

BAC-JPH3 and BAC-JPH3b6 mice express *JPH3* mRNA at levels comparable to that found in BAC-HDL2-F line mice (Figure S1; data not shown).

Phenotypic studies of both BAC-JPH3 and BAC-JPH3b6 control mice did not reveal any evidence of disease pathogenesis. First, BAC-JPH3 mice did not exhibit any rotarod deficits at 3 or 6 months old and their brains did not show 3B5H10-immunoreactive polyQ NIs at 14–18 months old (Figure S4B). Second, brain sections from 18- to 22-month-old BAC-JPH3b6 mice were not positively stained for ubiquitin or polyQ NIs (Figure S4B). To ascertain that the lack of NI phenotype in BAC-JPH3 control mice was not due to the relatively low level of transgene expression compared to the BAC-HDL2 line (~20%), we also assessed NI formation in the BAC-HDL2-F line, which has comparable levels of transgene expression to the BAC-JPH3 control mouse lines. As shown in Figure S4C, 3B5H10-immunoreactive NIs were readily detected in the cortex and hippocampus of 22-month-old BAC-HDL2-F line mice. Together, our analyses demonstrate that disease pathogenesis in HDL2 mice is dependent on CTG/CAG repeat expansion in the BAC transgene.

#### A Promoter Drives the Expression of an Antisense CAG Transcript Encoding an Expanded PolyQ Protein in BAC-HDL2 Mice

We next sought to address the molecular origin of the polyQ immunoreactivity within the NIs in BAC-HDL2 brains. Previously postulated sources of 1C2-immunoreactive NIs in HDL2 patients include: expression of a novel polyQ protein emanating from the strand antisense to the *JPH3* locus, expression of an expanded polyglutamine protein encoded by a CUG transcript, and sequestration of proteins with a long but nonpathogenic polyQ stretch such as TBP (Holmes et al., 2001; Margolis et al., 2005; Rudnicki et al., 2007). Studies conducted with limited patient brain samples could not definitively identify the source for the 1C2-immunoreactive NIs in HDL2 brains. In this study, we tested the hypothesis that NIs in HDL2 are due to the expression of a polyQ protein encoded by a *JPH3* antisense transcript containing an expanded CAG repeat.

Bioinformatic analyses performed on the antisense strand of the human *JPH3* locus revealed three ORFs that included the CAG-encoded polyQ stretch as well as several predicted downstream polyA signals (Figure 4A). To find evidence for the expression of such CAG transcripts, we used antisense-strand-specific and human-transcript-specific RT-PCR analyses (see Supplemental Experimental Procedures). These analyses readily detected the expression of antisense transcripts in BAC-HDL2 mouse brains, but not in wild-type controls (Figure 4B). In order to define the 5' and 3' regions of the transcript, we performed rapid amplification of cDNA ends (RACE). We were able to identify 5' RACE products encompassing the proximal two ATG codons in the polyQ ORF and 3' RACE revealed a polyA signal ~4kb from the repeat (data not shown). Similar antisense CAG transcripts were also detected in BAC-JPH3 control mice (see Figures 5D and 5E). This transcript, which we named *HDL2-CAG*, contains two translation-initiation codons (ATG) in frame with the polyQ-encoding CAG repeat. This protein contains a predicted ORF with 54 amino acids prior

to the polyQ repeat and 27 amino acids after the repeat (Figure 4A).

Because BAC-HDL2 mice express the *HDL2-CAG* transcript, we asked whether the genomic sequence preceding the polyQ ORF could possess promoter activity in primary neurons. To test this possibility, we subcloned three genomic DNA fragments consisting of 0.25, 0.5, and 1 kb of genomic DNA sequence preceding the *HDL2-CAG* ORF into a luciferase reporter construct (Figure 4C). The resulting constructs were transfected into primary cortical neurons to test their ability to drive luciferase transcription. Surprisingly, all three genomic fragments exhibited robust promoter activity in this assay (Figure 4C), suggesting that the promoter driving *HDL2-CAG* expression is located immediately preceding the polyQ ORF.

We next sought to provide direct evidence for the expression of a novel expanded polyQ protein consistent with the size of HDL2-CAG protein in BAC-HDL2 brains. We first experimentally determined the size of both mutant and wild-type HDL2-CAG protein by performing in vitro experiments where we expressed Flag-tagged HDL2-CAG protein with 120-CAG (HDL2-CAG<sub>120</sub>) or 14-CAG (HDL2-CAG<sub>14</sub>) repeats in HEK293 cells (Figure S5). Western blot analyses with 1C2 and 3B5H10 antibodies revealed that HDL2-CAG<sub>120</sub> protein in such transfected cells migrates as a doublet between 40 and 45kDa (Figure S5). HDL2-CAG<sub>14</sub>, which migrates at ~16kDa, is detected with the anti-Flag antibody and only marginally by the 1C2 antibody. Because 3B5H10 can selectively detect HDL2-CAG<sub>120</sub> protein in vitro, we performed western blot analyses by using fractionated brain extracts from 22-month-old BAC-HDL2 mice and wild-type controls. Immunoblotting with 3B5H10 antibody detected a doublet that migrated between 40 and 45kDa in BAC-HDL2 brains, but not wild-type control brains, consistent with the size of HDL2-CAG<sub>120</sub> protein in the in vitro experiments (Figure 4D). Interestingly, mutant HDL2-CAG protein can be robustly detected in insoluble nuclear fractions once the preparation has been solubilized by boiling in 2% SDS, but only a small, yet still detectable, amount of mutant HDL2-CAG can be found in the soluble nuclear fraction in the mutant, but not in wild-type, mouse brains (Figure 4D, long exposure).

In summary, we have demonstrated evidence for the expression of a CAG repeat-containing transcript in BAC-HDL2 mice, emanating from the strand antisense to the *JPH3* genomic locus. This expanded CAG transcript is driven by a promoter located immediately upstream of the polyQ ORF and is translated into an expanded polyQ protein in vivo.

#### Genetic Silencing of HDL2-CUG Transcripts Does Not Prevent the Expression of HDL2-CAG Transcripts and Polyglutamine Pathogenesis

Because genomic DNA immediately 5' to the *HDL2-CAG* ORF exhibits robust promoter activity, it raises the possibility that expression of the *HDL2-CAG* transcript and the resulting polyQ pathogenesis may be independent of the expression of *JPH3* sense strand transcripts and their protein products. To test this idea, we created a transgenic mouse model with a BAC construct replacing the *JPH3* exon 1 with GFP sequence followed by a transcriptional STOP sequence (Soriano, 1999), but still containing the expanded CTG/CAG repeats (~120 repeats) on

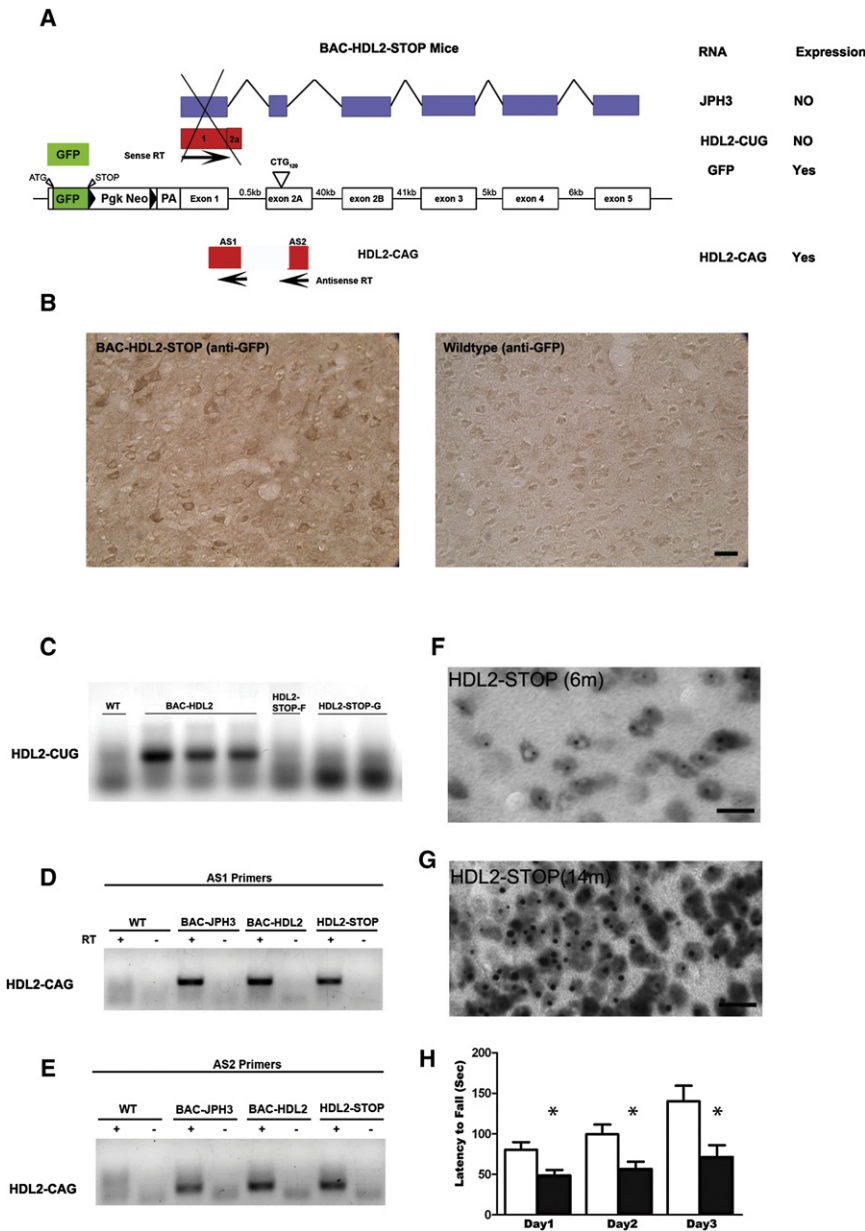


**Figure 5. Antisense HDL2-CAG Transcript and Accumulation of PolyQ Are Independent of the Expression of Sense Strand of *JPH3* Gene**

(A) A graphic representation of the construct of BAC-HDL2-STOP mice. A transcriptional STOP sequence consisting of GFP followed by triple polyadenylation signal was placed in front of the translation initiation codon of the exon 1 of the *JPH3* on the BAC transgene. This mouse line was designed to express GFP from *JPH3* promoter, but there is no transcription and translation of any other mRNA in the *JPH3* sense strand, including any of the transcripts that include the expanded CUG repeat.

(B) Anti-GFP antibody readily detected the expression of GFP protein in the cortical neurons in BAC-HDL2-STOP mice, but not in WT controls. (C) *JPH3* sense-strand-specific RT-PCR to amplify *HDL2-CUG* transcript revealed the expression of such transcript in BAC-HDL2 mice, but not in two lines of BAC-HDL2-STOP mice (lines F and G).

(D and E) Two independent strand-specific RT-PCR primer sets (AS1 and AS2 primers) specific to the *HDL2-CAG* transcripts readily detected the antisense CAG transcript in *JPH3*-FvB control mice, BAC-HDL2 mice, and BAC-HDL2-STOP mice.

(F and G) 3B5H10 immunostaining reveals progressive accumulation of polyQ NIs in cortical neurons of 6- and 12- month-old BAC-HDL2-STOP mice, but such NIs were not detected in the same brain region in the wild-type littermates (data not shown).

(H) Rotarod deficits in 12-month-old BAC-HDL2-STOP mice compared to wild-type controls. Significant deficits were detected on all 3 testing days. Values are mean  $\pm$  SEM ( $p < 0.05$ , Student's t test). Repeated-measure ANOVA analysis revealed a significant effect of time ( $F_{(2,8)} = 9.250$ ,  $p < 0.0001$ ), genotype ( $F_{(2,8)} = 9.331$ ,  $p = 0.009$ ), and interaction of time and genotype ( $F_{(2,8)} = 3.026$ ,  $p < 0.0001$ ). Scale bar = 50  $\mu$ m.

the BAC (Figure 5A). The STOP sequence, consisting of a floxed *neo* cassette followed by triple polyA signals, is a classic DNA sequence used to terminate transcription (Soriano, 1999; Srinivas et al., 2001). The resulting two mouse lines (F and G of BAC-HDL2-STOP mice) should express only GFP driven by the *JPH3* promoter, but no other sense strand CUG repeat or *JPH3* transcripts should be expressed (Figure 5A). On the other hand, the STOP sequence should not interfere with the transcription of the antisense *HDL2-CAG* transcripts; hence the model is still predicted to manifest polyQ pathogenesis.

To confirm the silencing of the sense strand transcripts, we first showed the expression of GFP protein in the BAC-HDL2-STOP, but not wild-type brains, by immunohistochemistry (Figure 5B). By using sense-strand-specific RT-PCR, we were able

to confirm that *HDL2-CUG* transcripts are indeed silenced in the BAC-HDL2-STOP mice (both F and G lines) as compared to the BAC-HDL2 mice (Figure 5C). Conversely, RT-PCR performed by using two separate antisense-strand-specific primers readily detected HDL2-CAG transcripts in the brains of BAC-HDL2-STOP mice as well as BAC-HDL2 and BAC-JPH3 mice (Figures 5D and 5E). These analyses confirmed that the STOP sequence successfully silenced the expression of *JPH3* and *HDL2-CUG* transcripts while leaving HDL2-CAG expression unperturbed in BAC-HDL2-STOP mice.

We next asked whether BAC-HDL2-STOP mice would develop NIs in vivo. Immunohistochemistry with 3B5H10 readily detected the progressive formation of polyQ NIs in BAC-HDL2-STOP mice (G line) between 6 and 14 months old,

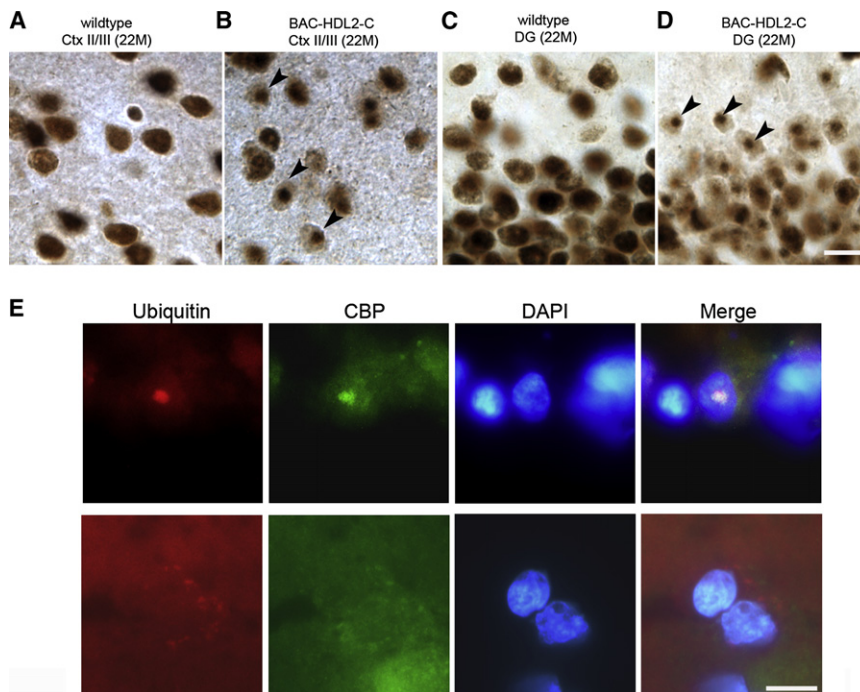


**Figure 6. CBP Sequestration in NIs in BAC-HDL2 Mice and HDL2 Patient Brains**

(A–D) Two anti-CBP antibodies (A-22 and sc-583) were used to confirm the presence of CBP-immunoreactive NIs in BAC-HDL2 mice (sc-583 is shown). Representative images of CBP staining of the superficial cortical layers (cortical layers II/III, A and B) and hippocampal dentate gyrus (DG, C and D) for wild-type (A and C) and BAC-HDL2 (B and D) sections are shown. Selected NIs are highlighted with black arrowheads.

(E) Double immunofluorescence staining with anti-CBP and anti-ubiquitin antibodies revealed the presence of CBP-immunoreactive NIs that colocalize with ubiquitin staining in the nucleus (DAPI staining) in the cortical cells in HDL2 postmortem brain. Cortical neurons in control brains do not have CBP and ubiquitin-immunoreactive NIs and CBP is diffusely distributed. Scale bar = 50 μm.

#### Sequestration of CBP and Functional Interference of CBP-Mediated Transcription in HDL2 Mice and Patients

We next explored whether NIs in BAC-HDL2 could exhibit other molecular

features similar to polyQ disorders including HD (Orr and Zoghbi, 2007). One such molecular marker that has been observed in several polyQ disorders (e.g., HD, SBMA, and SCA3) is the sequestration of polyQ domain-containing nuclear transcription factors in NIs, such as the potent transcription coactivator CBP (Kazantsev et al., 1999; Nucifora et al., 2001; McCampbell et al., 2000). We tested this possibility by immunohistochemical staining for CBP with 22-month-old BAC-HDL2 and control brain sections. In wild-type brains, we detected the characteristic diffuse CBP staining in nuclei throughout the brain (Figures 6A and 6C). However, in BAC-HDL2 brains, we detected the presence of CBP-immunoreactive NIs and a corresponding reduction of diffuse nuclear CBP staining in cortical and hippocampal neurons (Figures 6B and 6D). Occasionally, CBP-immunoreactive NIs could also be detected in the striatum (data not shown). The formation of CBP NIs is time dependent as they were initially detected at 12 months old, but not at 3 months old (data not shown). Thus, the sequestration of CBP in NIs occurred after the formation of polyQ NIs (first detected at 3 months old). Consistent with the hypothesis that CBP pathology is mediated by mutant HDL2-CAG protein, we did not detect any CBP inclusions in 18 to 22 month-old BAC-JPH3 (Figure S4A) or BAC-JPH3b6 controls (Figure S4B). As expected, silencing sense strand transcript in BAC-HDL2-STOP mice did not prevent CBP inclusion formation (Figure S6A).

To provide further evidence that the CBP pathology identified in BAC-HDL2 mice is relevant to HDL2 patients, we performed double immunofluorescent staining of HDL2 patient cortical tissue with anti-CBP and anti-ubiquitin antibodies. As shown in Figure 6E, we were able to detect CBP-immunoreactive NIs that colocalized with ubiquitin-immunoreactive NIs in the

but not in wild-type controls (Figures 5F and 5G; data not shown). Similar to those in BAC-HDL2, the NIs in BAC-HDL2-STOP mice were particularly abundant in the cortex and hippocampus and diffuse nuclear accumulation could also be detected in the striatum (Figure S6A).

We next addressed whether the selective expression of the mutant *HDL2-CAG* transcripts, but not *HDL2-CUG* or *JPH3* transcripts, is sufficient to elicit motor deficits and/or neurodegenerative pathology. As shown in Figure 5H, BAC-HDL2-STOP mice exhibit a significant accelerating rotarod deficit at 12 months old ( $n = 8$  per genotype;  $p < 0.05$  for each of the 3 testing days with Student's *t* test). Repeated-measures ANOVA analysis reveals a significant effect of time ( $F_{(2,8)} = 9.250$ ,  $p < 0.0001$ ), genotype ( $F_{(2,8)} = 9.331$ ,  $p = 0.009$ ), and interaction of time and genotype ( $F_{(2,8)} = 3.026$ ,  $p < 0.0001$ ), suggesting that mutant mice exhibit both motor performance and motor learning deficits in the rotarod test. To assess whether BAC-HDL2-STOP transgenic mice also show evidence of neurodegenerative pathology similar to that in BAC-HDL2 mice, we weighed forebrains and cerebella of the mutant and wild-type mice at 12 months old ( $n = 8$  per genotype). We did not detect any significant reduction of forebrain or cerebellar weight in mutant mice at this age (Figure S6B). These results show that the selective expression of mutant HDL2-CAG transcripts, but not *HDL2-CUG* transcripts, is sufficient to elicit neuronal dysfunction (e.g., rotarod deficits), but not yet sufficient to induce neurodegeneration at 12 months old.

In conclusion, the BAC-HDL2-STOP model provides definitive mouse genetic evidence that selective expression of *HDL2-CAG* transcript without coexpression of *JPH3* or *HDL2-CUG* transcript is sufficient to elicit polyQ pathogenesis and neuronal dysfunction in vivo.

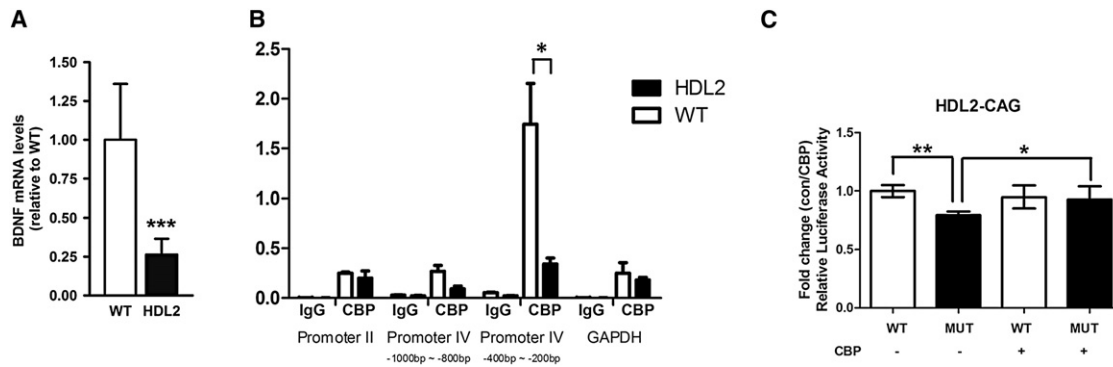


**Figure 7. CBP-Mediated Transcriptional Dysregulation in Mouse and Primary Neuronal Models of HDL2**

(A) Quantitative RT-PCR analyses of the intact *BDNF* coding region reveal a significant reduction of *BDNF* transcripts in 15-month-old BAC-HDL2 mice relative to wild-type control mice ( $n = 3$  per genotype;  $***p < 0.01$ , Student's *t* test). Values are mean  $\pm$  SEM.

(B) CBP occupancy of mouse *BDNF* promoter II, promoter IV (proximal region: 200–400 bp from the transcription start site; distal region: 800–1000 bp from the start site), *BDNF* coding region, and *GAPDH* promoter were determined by ChIP-PCR in cortical samples derived from wild-type and BAC-HDL2 mice at 15 months old ( $n = 3$  per genotype). ChIP-qPCR (IP/whole-cell extract, %) signals were normalized to whole-cell extract. Immunoprecipitation with IgG was used for controls. Error bars represent SEM determined from three independent experiments. The results suggest a significant and selective reduction of CBP binding to the proximal *BDNF* promoter IV (200–400 bp) in cortical samples from mutant BAC-HDL2 mice compared to WT controls. Values are mean  $\pm$  SEM ( $*p < 0.01$ , Student's *t* test).

(C) Luciferase reporter assays were performed in rat cortical primary neurons with cotransfection of *BDNF* promoter IV-driven firefly luciferase reporter construct and vectors expressing either HDL2-CAG14 (wild-type HDL2-CAG protein with 14 glutamine repeats, labeled WT) or HDL2-CAG120 (mutant protein with 120 glutamine repeats, labeled MUT). A separate set of transfection assays was performed with the same plasmids as above but with the addition of plasmids overexpressing CBP (labeled CBP +). A renilla luciferase expression plasmid was used to normalize transfection efficiency in all the assays. Values are mean  $\pm$  SEM ( $**p < 0.01$ ,  $*p < 0.05$ , Student's *t* test).

superior frontal gyri of two postmortem HDL2 brains, but not in the brains of unaffected controls.

CBP is a histone acetyltransferase and a critical transcriptional coactivator (Chan and La Thangue, 2001) and CBP sequestration and transcriptional interference has been implicated in HD pathogenesis (Nucifora et al., 2001; Steffan et al., 2001). To assess evidence of CBP functional impairment in HDL2, we decided to use CBP-mediated *BDNF* gene transcription as a model. *BDNF* is a critical trophic factor for striatal neurons and its transcriptional downregulation has been implicated in HD pathogenesis (reviewed by Zuccato et al., 2010). Moreover, our analyses of *BDNF* transcription by using quantitative RT-PCR analysis confirmed a significant reduction of transcripts containing the entire *BDNF* coding region in 15-month-old BAC-HDL2 cortices compared to those in the wild-type controls (Figure 7A).

We next addressed whether this *BDNF* transcriptional deficit in BAC-HDL2 could in part be due to functional interference of CBP. Transcription of *BDNF* is initiated at multiple promoters (Hong et al., 2008). In HD, there is evidence that transcription is reduced at both *BDNF* promoter II (Zuccato et al., 2001) and promoter IV (Gambazzi et al., 2010; Gray et al., 2008). Relevant to the current study *BDNF* promoter IV is regulated by neuronal activity and targeted by CREB and CBP (Hong et al., 2008). We hypothesized that mutant HDL2-CAG may interfere with CBP function and therefore could alter the transcription from *BDNF* promoter IV. To test this hypothesis, we used 15-month-old BAC-HDL2 and wild-type cortical extracts to perform chromatin immunoprecipitation (ChIP) experiments to quantify the amount of CBP bound to proximal versus distal regions of *BDNF* promoter IV by using *BDNF* promoter II as well as *GAPDH*

promoter regions as controls (Martinowich et al., 2003). As shown in Figure 7B, we found a significant and selective reduction in the amount of CBP bound to the proximal region of *BDNF* promoter IV in BAC-HDL2 cortical samples compared to those from wild-type controls. Such a difference was not observed in the distal region of *BDNF* promoter IV, in the control *BDNF* promoter II, or in the *GAPDH* promoter. Consistent with this finding, we also detected a decrease in histone H4 acetylation (H4Ac), an epigenetic marker of transcriptionally active chromatin, in the *BDNF* promoter IV in the BAC-HDL2 cortical samples compared to the wild-type controls (Figure S7). However, we did not observe any significant changes of other histone markers such as H3K4me3 or H3K27me3 (Martinowich et al., 2003).

Finally, to further explore in a primary neuron model whether CBP could functionally modify HDL2-CAG-mediated transcriptional dysregulation of *BDNF* promoter IV, we cotransfected primary cortical neurons with a reporter plasmid containing *BDNF* promoter IV-driven firefly luciferase and plasmids expressing either mutant (120 CAG repeats) or wild-type (14 CAG repeats) Flag-tagged HDL2-CAG proteins (Figure 7C and Figure S5). At 24 hr posttransfection, when we did not detect any significant cell death (data not shown), we found that mutant, but not wild-type, HDL2-CAG can induce significant reduction of firefly luciferase activity relative to the control renilla luciferase activity, suggesting that expression of mutant, but not wild-type, HDL2-CAG can interfere with *BDNF* promoter IV transcriptional activities (Figure 7C). Importantly, cotransfection of CBP can rescue such polyQ-length-dependent interference of transcription in this primary neuron model (Figure 7C).

In summary, our analyses of HDL2 models in primary neurons, mice, and patients provide converging evidence to support

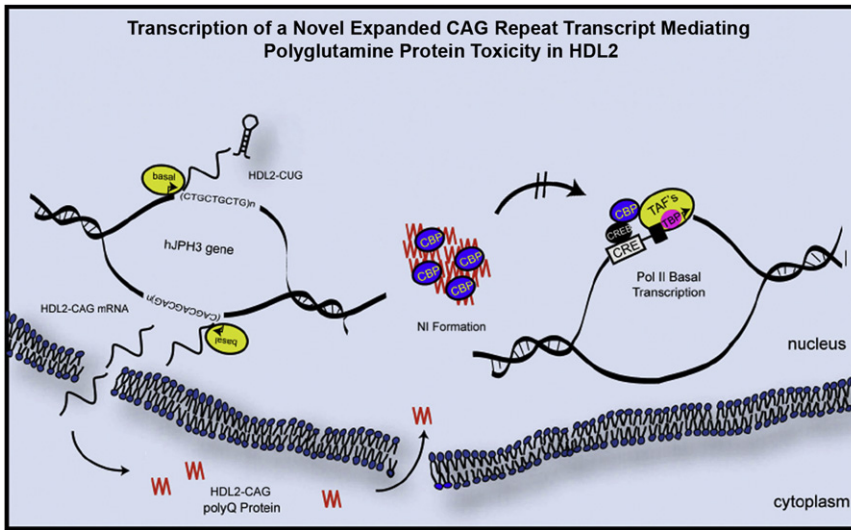


**Figure 8. A Schematic Model for Pathogenic Mechanisms Revealed by HDL2 Mouse Model in which an Antisense Expanded CAG Transcript Is Mediating PolyQ Pathogenesis In Vivo**

An expanded CAG repeat (*HDL2-CAG*) antisense to the *JPH3* sense strand is transcribed from its own promoter immediately 5' to the CAG repeat and the transcript is then translated into an expanded polyQ protein termed HDL2-CAG. Mutant HDL2-CAG is translocated and accumulated in the nucleus to form prominent NIs consisting of HDL2-CAG protein, ubiquitin, and at a later time point, CBP. Transcriptional dysregulation, in part from interference of CBP-mediated activation of gene expression (e.g., *BDNF*), may be a shared molecular pathogenic mechanism between HD and HDL2.

polyQ-length-dependent CBP sequestration and functional interference of CBP-mediated transcription in HDL2.

## DISCUSSION

We have generated and characterized BAC transgenic mouse models of an HD-like disorder, HDL2. BAC-HDL2 mice recapitulate several key phenotypes found in HDL2 patients, including age-dependent motor deficits and selective forebrain atrophy. They also capture two molecular pathogenic hallmarks of HDL2: the progressive accumulation of ubiquitin-positive NIs and the presence of CUG-containing RNA foci that are not colocalized with NIs. Importantly, this model reproduces the brain region-specific distribution of NIs seen in the patients, suggesting that the mechanism underlying the pathogenesis of NIs is probably reproduced in this mouse model. Furthermore, the disease phenotypes are not present in control BAC mice without the CTG/CAG repeat expansion.

Our study provides insight into the molecular mechanism leading to polyQ pathogenesis in BAC-HDL2 mice (see schematics in Figure 8). By using a series of BAC transgenic mouse models, we demonstrated the expression of an expanded CAG-containing transcript from the strand antisense to *JPH3*, with its expression driven by a novel promoter. Second, immunohistochemistry and western blot analyses demonstrated that this transcript is expressed as a protein containing an expanded polyQ tract. Third, we used two antibodies relatively specific for polyQ to demonstrate the accumulation of NIs containing polyQ in two independent lines of BAC-HDL2 mice and found the spatial distribution of NI accumulation to be strikingly similar to that found in HDL2 patients. Fourth, we used two control BAC mouse lines with normal CTG/CAG repeats to demonstrate that disease pathogenesis in BAC-HDL2 mice, including NI formation, is dependent on the CTG/CAG repeat expansion. Finally, by genetic silencing of the *JPH3* sense strand in BAC-HDL2-STOP mice, preventing expression of CUG-containing transcripts, we provided definitive genetic evidence that the

expression of the *HDL2-CAG* transcript alone can lead to the formation of polyQ-containing NIs and manifestation of motor deficits. Taken together, our analyses of the series of HDL2 mouse models provide an important mechanistic insight that the expression of a novel expanded polyQ protein could play a critical role in HDL2 pathogenesis in vivo.

Prior to this study, the expression of an expanded antisense CAG-containing transcript or a novel polyQ protein had not been demonstrated by using postmortem patient brain tissues (Holmes et al., 2001; Margolis et al., 2005). There are several possible explanations to account for the more sensitive detection of the CAG transcript and polyQ-expanded protein in HDL2 mice than in patients. First, unlike the postmortem brain tissues, the HDL2 mouse brains used for the studies do not exhibit robust neurodegeneration that may lead to the loss of neurons expressing mutant CAG transcripts at high levels. Second, the sequence difference between the human mutant *JPH3* transgene and murine wild-type locus in the same HDL2 mouse permits the easier detection of the mutant antisense transcripts. Third, the much longer polyQ repeat in the BAC-HDL2 mouse model (120Q, as compared to 40–50Q in patients) also permits more sensitive detection of the small amount of soluble mutant polyQ protein with antibodies that provide signal strength in western blots depending on the polyQ length (e.g., 3B5H10). Because the brain regional and subcellular distribution of the NIs are remarkably similar between HDL2 mice and patients, it would strongly argue that the molecular pathogenesis for such NIs in HDL2 mice and patients is also likely to be similar. Future studies with additional patient samples and more sensitive detection methods may be needed to demonstrate *HDL2-CAG* transcript and protein in the patient brains.

Although our study is focused on the mechanistic investigation of the novel antisense CAG repeat transcript and its polyQ-containing protein product, our study does not exclude a contribution of other potential mechanisms to aspects of HDL2 pathogenesis, such as partial loss of *JPH3* function or CUG repeat RNA gain-of-function toxicity (Rudnicki et al., 2007).

Despite the fact that our study was not designed to address these alternative mechanisms, our models do support a potential role of CUG RNA in disease pathogenesis, because BAC-HDL2 mice accumulate CUG RNA foci that can sequester Mbn1, hence mimicking those molecular pathological hallmarks in the patients. Importantly, the CUG RNA foci and NIs in both HDL2 mice and patients appear to be distinct entities, consistent with the interpretation that independent pathogenic mechanisms lead to their formation (Rudnicki et al., 2007; Figure S2B). Because expanded CUG repeat RNA is clearly pathogenic in DM1 via an RNA gain-of-function mechanism (Mankodi et al., 2001), in part via sequestration and depletion of MBNL1 (Kana-dia et al., 2003), future mouse genetic studies are needed to address whether the expression of expanded CUG repeat transcripts also could mediate CUG repeat RNA toxicities in vivo.

An overarching goal of this study was to shed light on potential common pathogenic mechanisms shared between HD and HD-like disorders. By the development and analysis of the BAC mouse genetic model for an HD-like disorder, we have already gained some initial insights toward this important objective. First, our cumulative analysis of these models suggests that expanded polyQ-mediated pathogenesis may be a shared pathogenic mechanism between HD and HDL2. The finding that a mutant polyQ protein may contribute to HDL2 pathogenesis in BAC-HDL2 mice is consistent with the presence of NIs that are immunostained with both 1C2 and 3B5H10 antibodies in HDL2 brain and the comparable pathogenic CAG repeat threshold for HDL2 and HD (about 40 triplets). It is striking that this threshold is similar to other polyglutamine diseases, but is much shorter than the threshold for most of the nonpolyglutamine repeat expansion disorders, most prominently DM1. Thus, our study provides experimental evidence to suggest that therapeutics that ameliorate expanded polyQ toxicity could benefit those with both HD and HDL2.

Another potentially shared pathogenic mechanism between HD and HDL2 is transcriptional dysregulation mediated by sequestration and/or functional interference of CBP. Prior studies have demonstrated that mutant huntingtin N-terminal fragments can bind to and/or sequester CBP into aggregates, leading to changes in CBP-mediated transcription (Kazantsev et al., 1999; Nucifora et al., 2001; Steffan et al., 2000). Although physical depletion of CBP is not consistently observed in all HD mouse models (Yu et al., 2002), functional interference of CBP has been observed in HD as well as other polyQ disorders. Indirect restoration of CBP function via histone deacetylase inhibition has been shown to be beneficial in several animal models of HD (Steffan et al., 2001) and in other polyQ disorders such as SBMA (McCampbell et al., 2000; Taylor et al., 2003). Our analysis of BAC-HDL2 mice provides evidence that expression of BDNF is significantly reduced in the mutant cortex at 15 months old, and our in vivo ChIP analysis and primary neuron study reveal that mutant HDL2-CAG can selectively interfere with CBP coactivator function at *BDNF* promoter IV (Hong et al., 2008). Our study supports the notion that mutant HDL2-CAG protein can perturb CBP-mediated transcription, in part, but not necessarily exclusively, through the sequestration of CBP into NIs. Our current study does not rule out the possibility that mutant HDL2-CAG protein may also disrupt the function of other critical

nuclear transcription factors such as TBP (Rudnicki et al., 2008). Additional gene expression and epigenetic profiling, along with functional manipulation of these molecular pathways in HDL2 mice, will be necessary to critically evaluate their contribution in disease pathogenesis.

Finally, our study reveals the complexity of disease pathogenesis mediated by trinucleotide repeat expansion. Together with SCA8 (Moseley et al., 2006), our models provide another compelling example in which bidirectional transcription across an expanded CTG/CAG repeat leads to the expression of an antisense CAG transcript and previously unrecognized polyQ protein toxicity. Because the predicted HDL2-CAG protein has no known homology to any other protein in the human proteome beyond the polyQ stretch (data not shown), the function of this transcript and the small protein it encodes remains to be explored. Given the recent discovery that antisense transcription is nearly ubiquitous throughout the mammalian genome (Katayama et al., 2005), our study highlights the importance of examining antisense repeat-containing transcripts and their ORFs in the pathogenesis of other brain disorders.

## EXPERIMENTAL PROCEDURES

### Generation of BAC Transgenic Mouse Models of HDL2

Human BAC (RP11-33A21) containing the *JPH3* genomic locus from BACPAC Resource Center (Oakland Children's Hospital, Oakland, CA) was engineered by using homologous recombination and microinjected into FvB/N embryos to generate the BAC transgenic mouse lines, BAC-HDL2, BAC-HDL2-STOP, and BAC-JPH3 (Yang et al., 1997; Gong et al., 2002). These mouse lines were maintained in FvB/NJ inbred background. A second BAC control mouse that was generated by using the wild-type *JPH3* BAC (CTD-2195P9) was created and maintained in the C57/BL6 background (BAC-JPH3b6). More details about the transgene constructs and initial characterization of the mouse lines are in Supplemental Experimental Procedures.

### Reverse Transcriptase PCR Analyses of Strand-Specific RNA Expression

For RT-PCR analyses of *JPH3* sense strand and antisense *HDL2-CAG* transcripts, total RNA was extracted by using the RNeasy Lipid mini-kit (QIAGEN, Valencia, CA). Synthesis of cDNA was primed by using either oligo(dT)<sub>20</sub> (Invitrogen, Carlsbad, CA) or strand-specific oligonucleotide primers (see Table S1 for primers). Both 5' and 3' RACE analyses were performed by using FirstChoice® RLM-RACE kit (ABI) following the manufacturer's instructions. A random-primed reverse transcription reaction and nested PCR was used to amplify 5' and 3' ends of the transcript (see Table S1). Quantitative RT-PCR analyses of *BDNF* transcripts in BAC-HDL2 and control cortices were performed by using published protocol (Gray et al., 2008).

### Accelerating Rotarod, Brain Weights, and Stereological Measurement of Brain Volumes

See published protocols for the rotarod, forebrain and cerebellar weights, and stereological measurement of cortical and striatal volumes (Gray et al., 2008; Gu et al., 2009; see Supplemental Experimental Procedures).

### Immunohistochemistry

Mouse brains were perfused, sectioned, and immunostained by using established protocols (Gray et al., 2008; Gu et al., 2009; see Supplemental Experimental Procedures). HDL2 brain samples used in the study were described in detail before (Rudnicki et al., 2008). The following antibodies were used to stain NIs in HDL2 models: 3B5H10 (1:1000; Sigma, St. Louis, MO), 1C2 (1:3000; Chemicon, Billerica, MA), CBP (1:3000; A-22 & sc-583, Santa Cruz, Santa Cruz, CA), ubiquitin (1:1000; DakoCytomation, Carpinteria, CA), 3B5H10 (1:2000), MBNL1 antibody (A2764, 1:10000 dilution; Lin

et al., 2006). Antigen retrieval for polyQ NI detection by using 3B5H10 was performed according to published protocols (Osmand et al., 2006). More details on immunohistochemical methods and reagents and quantitation of NI sizes can be found in Supplemental Experimental Procedures.

#### Western Blotting

Brain extracts or nuclear and cytoplasmic fractionations were performed by using established methods (Gray et al., 2008; Gu et al., 2009; see Supplemental Experimental Procedures). Antibodies for western blot included: JPH3 exon 4 (1:1000; H. Takeshima, Tohoku University, Japan), M2-Flag (1:500),  $\alpha$ -tubulin (1:2000), 3B5H10 (1:1000; Sigma, St. Louis, MO), and 1C2 (1:2000; Chemicon, Billerica, MA).

#### Chromatin Immunoprecipitation

ChIP analyses were performed by using our established method (Martinowich et al., 2003; see Supplemental Experimental Procedures) with the following antibodies: anti-CBP (sc-583, Santa Cruz) and anti-IgG (sc-66931, Santa Cruz). Real-time quantitative PCR was performed by using iQ SYBR Green Supermix (Bio-Rad). For quantification of relative level of CBP occupancy, we calculated the percentage of immunoprecipitated DNA over whole-cell extract. Primer sequences used in ChIP-qPCR are listed in Supplemental Experimental Procedures.

#### DNA Constructs, Cortical Primary Neuron Culture, Transfection, and Luciferase Reporter Assays

See details in Supplemental Experimental Procedures.

#### Statistical Analysis

All data are shown as the mean  $\pm$  SEM. SPSS 14.0 statistics software (SPSS, Chicago, IL) was used to perform all statistical analyses. The significance level was set at 0.05. See more details in Supplemental Experimental Procedures and in our published methods (Gray et al., 2008; Gu et al., 2009).

#### SUPPLEMENTAL INFORMATION

Supplemental Information includes seven figures, one table, and Supplemental Experimental Procedures and can be found with this article online at doi:10.1016/j.neuron.2011.03.021.

#### ACKNOWLEDGMENTS

This work was generously supported by independent research grants from the Hereditary Disease Foundation to X.W.Y., R.L.M., A.O., and to D.D.R. X.W.Y. is also supported by National Institutes of Health (NIH)/National Institute of Neurological Disorders and Stroke (NINDS; R01NS049501), the David Weil Fund to the Semel Institute at University of California, Los Angeles, and Neuroscience of Brain Disorders Award from The McKnight Endowment Fund for Neuroscience. R.L.M. and D.D.R. are supported by NIH/NINDS (R21NS057516 and R01NS064138). We would like to thank N.S. Wexler and C. Johnson for their tremendous support of this project. We also thank members of the Yang lab for discussions and reading of the manuscript. B.W. and C.S.P. were supported by predoctoral fellowships from the UCLA Center for Neurobehavioral Genetics Predoctoral Training Program funded by National Institute of Mental Health (5T32MH073526).

Accepted: March 28, 2011

Published: May 11, 2011

#### REFERENCES

Brooks, E., Arrasate, M., Cheung, K., and Finkbeiner, S.M. (2004). Using antibodies to analyze polyglutamine stretches. *Methods Mol. Biol.* 277, 103–128.

Chan, H.M., and La Thangue, N.B. (2001). p300/CBP proteins: HATs for transcriptional bridges and scaffolds. *J. Cell Sci.* 114, 2363–2373.

Dorsman, J.C., Peppers, B., Langenberg, D., Kerkdijk, H., Ijszenga, M., den Dunnen, J.T., Roos, R.A., and van Ommen, G.J. (2002). Strong aggregation

and increased toxicity of polyleucine over polyglutamine stretches in mammalian cells. *Hum. Mol. Genet.* 11, 1487–1496.

Gambazzi, L., Gokce, O., Seredenina, T., Katsyuba, E., Runne, H., Markram, H., Giugliano, M., and Luthi-Carter, R. (2010). Diminished activity-dependent brain-derived neurotrophic factor expression underlies cortical neuron microcircuit hypoconnectivity resulting from exposure to mutant huntingtin fragments. *J. Pharmacol. Exp. Ther.* 335, 13–22.

Gong, S., Yang, X.W., Li, C., and Heintz, N. (2002). Highly efficient modification of bacterial artificial chromosomes (BACs) using novel shuttle vectors containing the R6Kgamma origin of replication. *Genome Res.* 12, 1992–1998.

Gray, M., Shirasaki, D.I., Cepeda, C., André, V.M., Wilburn, B., Lu, X.H., Tao, J., Yamazaki, I., Li, S.H., Sun, Y.E., et al. (2008). Full-length human mutant huntingtin with a stable polyglutamine repeat can elicit progressive and selective neuropathogenesis in BACHD mice. *J. Neurosci.* 28, 6182–6195.

Greenstein, P.E., Vonsattel, J.P., Margolis, R.L., and Joseph, J.T. (2007). Huntington's disease like-2 neuropathology. *Mov. Disord.* 22, 1416–1423.

Gu, X., Greiner, E.R., Mishra, R., Kodali, R., Osmand, A., Finkbeiner, S., Steffan, J.S., Thompson, L.M., Wetzler, R., and Yang, X.W. (2009). Serines 13 and 16 are critical determinants of full-length human mutant huntingtin induced disease pathogenesis in HD mice. *Neuron* 64, 828–840.

Holmes, S.E., O'Hearn, E., Rosenblatt, A., Callahan, C., Hwang, H.S., Ingersoll-Ashworth, R.G., Fleisher, A., Stevanin, G., Brice, A., Potter, N.T., et al. (2001). A repeat expansion in the gene encoding junctophilin-3 is associated with Huntington disease-like 2. *Nat. Genet.* 29, 377–378.

Hong, E.J., McCord, A.E., and Greenberg, M.E. (2008). A biological function for the neuronal activity-dependent component of Bdnf transcription in the development of cortical inhibition. *Neuron* 60, 610–624.

Kanadia, R.N., Johnstone, K.A., Mankodi, A., Lungu, C., Thornton, C.A., Esson, D., Timmers, A.M., Hauswirth, W.W., and Swanson, M.S. (2003). A muscleblind knockout model for myotonic dystrophy. *Science* 302, 1978–1980.

Katayama, S., Tomaru, Y., Kasukawa, T., Waki, K., Nakanishi, M., Nakamura, M., Nishida, H., Yap, C.C., Suzuki, M., Kawai, J., et al; RIKEN Genome Exploration Research Group; Genome Science Group (Genome Network Project Core Group); FANTOM Consortium. (2005). Antisense transcription in the mammalian transcriptome. *Science* 309, 1564–1566.

Kazantsev, A., Preisinger, E., Dranovsky, A., Goldgaber, D., and Housman, D. (1999). Insoluble detergent-resistant aggregates form between pathological and nonpathological lengths of polyglutamine in mammalian cells. *Proc. Natl. Acad. Sci. USA* 96, 11404–11409.

Lin, X., Miller, J.W., Mankodi, A., Kanadia, R.N., Yuan, Y., Moxley, R.T., Swanson, M.S., and Thornton, C.A. (2006). Failure of MBNL1-dependent post-natal splicing transitions in myotonic dystrophy. *Hum. Mol. Genet.* 15, 2087–2097.

Mankodi, A., Urbinati, C.R., Yuan, Q.P., Moxley, R.T., Sansone, V., Krym, M., Henderson, D., Schalling, M., Swanson, M.S., and Thornton, C.A. (2001). Muscleblind localizes to nuclear foci of aberrant RNA in myotonic dystrophy types 1 and 2. *Hum. Mol. Genet.* 10, 2165–2170.

Margolis, R.L., O'Hearn, E., Rosenblatt, A., Willour, V., Holmes, S.E., Franz, M.L., Callahan, C., Hwang, H.S., Troncoso, J.C., and Ross, C.A. (2001). A disorder similar to Huntington's disease is associated with a novel CAG repeat expansion. *Ann. Neurol.* 50, 373–380.

Margolis, R.L., Holmes, S.E., Rosenblatt, A., Gourley, L., O'Hearn, E., Ross, C.A., Seltzer, W.K., Walker, R.H., Ashizawa, T., Rasmussen, A., et al. (2004). Huntington's disease-like 2 (HDL2) in North America and Japan. *Ann. Neurol.* 56, 670–674.

Margolis, R.L., Rudnicki, D.D., and Holmes, S.E. (2005). Huntington's disease like-2: Review and update. *Acta Neurol. Taiwan.* 14, 1–8.

Martinowich, K., Hattori, D., Wu, H., Fouse, S., He, F., Hu, Y., Fan, G., and Sun, Y.E. (2003). DNA methylation-related chromatin remodeling in activity-dependent BDNF gene regulation. *Science* 302, 890–893.

McC Campbell, A., Taylor, J.P., Taye, A.A., Robitschek, J., Li, M., Walcott, J., Merry, D., Chai, Y., Paulson, H., Sobue, G., and Fischbeck, K.H. (2000).

- CREB-binding protein sequestration by expanded polyglutamine. *Hum. Mol. Genet.* **9**, 2197–2202.
- Moseley, M.L., Zu, T., Ikeda, Y., Gao, W., Mosemiller, A.K., Daughters, R.S., Chen, G., Weatherspoon, M.R., Clark, H.B., Ebner, T.J., et al. (2006). Bidirectional expression of CUG and CAG expansion transcripts and intranuclear polyglutamine inclusions in spinocerebellar ataxia type 8. *Nat. Genet.* **38**, 758–769.
- Nishi, M., Hashimoto, K., Kuriyama, K., Komazaki, S., Kano, M., Shibata, S., and Takeshima, H. (2002). Motor discoordination in mutant mice lacking junctophilin type 3. *Biochem. Biophys. Res. Commun.* **292**, 318–324.
- Nucifora, F.C., Jr., Sasaki, M., Peters, M.F., Huang, H., Cooper, J.K., Yamada, M., Takahashi, H., Tsuji, S., Troncoso, J., Dawson, V.L., et al. (2001). Interference by huntingtin and atrophin-1 with cbp-mediated transcription leading to cellular toxicity. *Science* **291**, 2423–2428.
- Orr, H.T., and Zoghbi, H.Y. (2007). Trinucleotide repeat disorders. *Annu. Rev. Neurosci.* **30**, 575–621.
- Osmand, A.P., Berthelot, V., and Wetzel, R. (2006). Imaging polyglutamine deposits in brain tissue. *Methods Enzymol.* **412**, 106–122.
- Ranum, L.P., and Cooper, T.A. (2006). RNA-mediated neuromuscular disorders. *Annu. Rev. Neurosci.* **29**, 259–277.
- Rudnicki, D.D., Holmes, S.E., Lin, M.W., Thornton, C.A., Ross, C.A., and Margolis, R.L. (2007). Huntington's disease—like 2 is associated with CUG repeat-containing RNA foci. *Ann. Neurol.* **61**, 272–282.
- Rudnicki, D.D., Pletnikova, O., Vonsattel, J.P., Ross, C.A., and Margolis, R.L. (2008). A comparison of huntington disease and huntington disease-like 2 neuropathology. *J. Neuropathol. Exp. Neurol.* **67**, 366–374.
- Schneider, S.A., Walker, R.H., and Bhatia, K.P. (2007). The Huntington's disease-like syndromes: What to consider in patients with a negative Huntington's disease gene test. *Nat. Clin. Pract. Neurol.* **3**, 517–525.
- Soriano, P. (1999). Generalized lacZ expression with the ROSA26 Cre reporter strain. *Nat. Genet.* **21**, 70–71.
- Srinivas, S., Watanabe, T., Lin, C.S., William, C.M., Tanabe, Y., Jessell, T.M., and Costantini, F. (2001). Cre reporter strains produced by targeted insertion of EYFP and ECFP into the ROSA26 locus. *BMC Dev. Biol.* **1**, 4.
- Steffan, J.S., Kazantsev, A., Spasic-Boskovic, O., Greenwald, M., Zhu, Y.Z., Gohler, H., Wanker, E.E., Bates, G.P., Housman, D.E., and Thompson, L.M. (2000). The Huntington's disease protein interacts with p53 and CREB-binding protein and represses transcription. *Proc. Natl. Acad. Sci. USA* **97**, 6763–6768.
- Steffan, J.S., Bodai, L., Pallos, J., Poelman, M., McCampbell, A., Apostol, B.L., Kazantsev, A., Schmidt, E., Zhu, Y.Z., Greenwald, M., et al. (2001). Histone deacetylase inhibitors arrest polyglutamine-dependent neurodegeneration in *Drosophila*. *Nature* **413**, 739–743.
- Takeshima, H. (2001). Junctophilins: Molecular components contributing junctional membrane complexes between the cell-surface membrane and endoplasmic/sarcoplasmic reticulum [in Japanese]. *Clin. Calcium* **11**, 758–762.
- Taylor, J.P., Taye, A.A., Campbell, C., Kazemi-Esfarjani, P., Fischbeck, K.H., and Min, K.T. (2003). Aberrant histone acetylation, altered transcription, and retinal degeneration in a *Drosophila* model of polyglutamine disease are rescued by CREB-binding protein. *Genes Dev.* **17**, 1463–1468.
- Trottier, Y., Lutz, Y., Stevanin, G., Imbert, G., Devys, D., Cancel, G., Saudou, F., Weber, C., David, G., Tora, L., et al. (1995). Polyglutamine expansion as a pathological epitope in Huntington's disease and four dominant cerebellar ataxias. *Nature* **378**, 403–406.
- Yang, X.W., Model, P., and Heintz, N. (1997). Homologous recombination based modification in *Escherichia coli* and germline transmission in transgenic mice of a bacterial artificial chromosome. *Nat. Biotechnol.* **15**, 859–865.
- Yu, Z.X., Li, S.H., Nguyen, H.P., and Li, X.J. (2002). Huntingtin inclusions do not deplete polyglutamine-containing transcription factors in HD mice. *Hum. Mol. Genet.* **11**, 905–914.
- Zoghbi, H.Y., and Botas, J. (2002). Mouse and fly models of neurodegeneration. *Trends Genet.* **18**, 463–471.
- Zuccato, C., Ciammola, A., Rigamonti, D., Leavitt, B.R., Goffredo, D., Conti, L., MacDonald, M.E., Friedlander, R.M., Silani, V., Hayden, M.R., et al. (2001). Loss of huntingtin-mediated BDNF gene transcription in Huntington's disease. *Science* **293**, 493–498.
- Zuccato, C., Valenza, M., and Cattaneo, E. (2010). Molecular mechanisms and potential therapeutic targets in Huntington's disease. *Physiol. Rev.* **90**, 905–981.